NACA

RESEARCH MEMORANDUM

FREE-FLIGHT INVESTIGATION, INCLUDING SOME EFFECTS OF WING

AEROELASTICITY, OF THE ROLLING EFFECTIVENESS OF AN

ALL-MOVABLE HORIZONTAL TAIL WITH DIFFERENTIAL

INCIDENCE AT MACH NUMBERS FROM 0.6 TO 1.5

By Roland D. English

Langley Aeronautical Laboratory
Langley Field, Va.

NATIONAL ADVISORY COMMITTEE
FOR AERONAUTICS

CONFIDENTIAL

NATIONAL ADVISORY COMMITTEE FOR AERONAUTICS

RESEARCH MEMORANDUM

FREE-FLIGHT INVESTIGATION, INCLUDING SOME EFFECTS OF WING

AEROELASTICITY, OF THE ROLLING EFFECTIVENESS OF AN

ALL-MOVABLE HORIZONTAL TAIL WITH DIFFERENTIAL

INCIDENCE AT MACH NUMBERS FROM 0.6 TO 1.5

By Roland D. English

SUMMARY

The Langley Pilotless Aircraft Research Division has made an investigation to determine the zero-lift rolling effectiveness of all-movable sweptback horizontal tail fins mounted behind a notched delta wing at a constant angle of differential incidence of 7° per fin. Two models, one with a stiff wing (solid aluminum alloy) and one with a flexible wing (fiber-glass—plastic laminate), were tested in free flight over a Mach number range from 0.6 to 1.5. The results indicate that the rolling effectiveness was of about the same magnitude at subsonic and supersonic speeds for both models. The rolling effectiveness of the flexible-wing model was about 1.6 times that of the stiff-wing model except in the transonic region.

INTRODUCTION

The ability of recent jet-propelled aircraft to reach supersonic speeds where conventional ailerons lose a large part of their effectiveness has made it necessary to consider other means of lateral control. Previous experience indicates that all-movable-type controls retain their effectiveness at supersonic speeds. Data are presented in reference 1 for the all-movable horizontal tail as a lateral control device at low speeds, but very little information is available on the all-movable tail at high subsonic and supersonic speeds. The Langley Pilotless Aircraft Research Division has made an investigation to determine the rolling effectiveness of an all-movable horizontal tail at a constant differential angle of incidence behind a notched delta wing over a range of Mach numbers from 0.6 to 1.5. Two rocket-propelled models, one with a stiff wing and one with a flexible wing, were tested in free flight at zero angle of attack. The experimental data from the model with the stiffer wing are compared with theoretical estimates.

CONFIDENTIAL

SYMBOLS

b	total wing span, ft
c	wing chord, ft
M	Mach number
m	twisting couple applied at $0.75b/2$ in a plane parallel to model center line and perpendicular to wing chord plane, in-lb
P	load applied at $0.75b/2$ on wing 40-percent-chord line in a direction perpendicular to wing chord plane, lb
p	rolling velocity, radians/sec
R	Reynolds number
V	model flight-path velocity, ft/sec
y	distance along span from model center line, ft
$pb/2V$	wing-tip helix angle, radians
$\dfrac{y}{b/2}$	nondimensional spanwise station
i_t	deflection of each horizontal tail fin (measured parallel to model center line) relative to model center line, deg
δ	deflection of wing 40-percent-chord line in a direction perpendicular to wing chord plane resulting from P, in.
θ	angle of wing twist in plane of and resulting from m, radians
δ/P	flexural-stiffness parameter, in./lb
θ/m	torsional-stiffness parameter, radians/in-lb
α	angle of attack, deg
β	angle of sideslip, deg

DESCRIPTION OF MODELS AND TESTS

The geometric details and dimensions of the test models are shown in the photograph of figure 1 and the sketch of figure 2. Both models had notched delta wings of aspect ratio 3.20, sweptback 55° at the leading edge and 10° at the trailing edge. Exposed wing area was 1.58 square feet, b/2 was 1.33 feet, and the wing airfoil section was the NACA 65A003 parallel to the free stream. The wing of model 1 was constructed of solid aluminum alloy and the wing of model 2 of a fiber-glass—plastic laminate. Structural-stiffness characteristics of the wings are shown in figure 3. The horizontal tail of each model had an aspect ratio of 4.00, a taper ratio of 0.60, a semispan of 0.67 foot, an exposed area of 0.28 square foot, the NACA 65A006 airfoil section parallel to the free stream, and was swept back 45° at the quarter-chord line. The horizontal tail fins were deflected differentially about a line through the 40-percent-chord at the fin body juncture perpendicular to the model center line. The deflection of each fin was 7°. Solid-aluminum-alloy construction was used for the horizontal tail fins of both models. The vertical tail had an aspect ratio of 3.16, a taper ratio of 0.12, a semispan of 0.63 foot, an exposed area of 0.24 square foot, and was swept back 45° at the leading edge. Vertical tail fins were made of 1/16-inch steel flat plate rounded at the leading edge.

The models were propelled to a Mach number of approximately 1.5 by two-stage rocket-propulsion systems. All test data were recorded at $\alpha = 0°$ during periods of free flight following burnout of the second propulsion stage. Rolling velocity, obtained by means of radio equipment (spinsondes), and model flight-path velocity and space coordinates, obtained by means of radar, were used with atmospheric data from radiosondes to calculate the variation of the rolling effectiveness parameter pb/2V with Mach number. The range of test Reynolds numbers is shown in figure 4. A description of the test method is given in more detail in reference 2.

ACCURACY AND CORRECTIONS

It is estimated that the test data are accurate within the following limits:

pb/2V . . . . ±0.004
M . . . . ±0.01

The pb/2V data have been corrected by the method of reference 3 for the wing- and tail-incidence errors resulting from construction tolerances. No correction was made for the effects of moment of inertia in roll since reference 2 shows this correction to be negligible.

RESULTS AND DISCUSSION

The variation of the rolling effectiveness parameter $pb/2V$ with Mach number is presented in figure 5. It may be seen from figure 5 that rolling effectiveness is about the same at subsonic and supersonic speeds for both models. The rolling effectiveness of the flexible-wing model was about 1.6 times that of the stiff-wing model except in the transonic region where a reduction in the rolling effectiveness of the flexible-wing model occurred. The higher rolling effectiveness of the flexible-wing model is undoubtedly due to the lower damping in roll of the flexible wing. The $pb/2V$ values of figure 5 would probably be sufficient at high subsonic and supersonic speeds, but are rather low in the low subsonic range. These $pb/2V$ values were obtained at zero lift, however, and reference 1 indicates that rolling effectiveness of the all-movable tail increases with increasing lift coefficient. Since at low speeds an airplane is usually operating at high lift coefficient, the rolling effectiveness of the all-movable tail would probably be higher than that of figure 5.

The ratio of tail area to wing area and the tail length of the models are fairly representative of present full-scale airplanes so the rolling effectiveness of the models should be a good estimate of the rolling effectiveness of a full-scale airplane with similar wing and tail plan forms and equivalent wing structural characteristics. Most full-scale airplane wings would probably be stiffer than the flexible wing but not as stiff as the stiff wing of the present investigation so the rolling effectiveness of a full-scale airplane would be somewhere between the rolling effectiveness of the stiff-wing model and the rolling effectiveness of the flexible-wing model. It should be noted that the data of this investigation are for a tail deflection of 7° per fin, and higher tail deflections are probably practicable.

Rolling effectiveness of the stiff-wing model is compared with theoretical estimates in figure 6. Theoretical rolling effectiveness was calculated using the strip theory of reference 3 and the modified lifting-line theory of reference 4. The presence of the body and wing-tail interference were neglected in the calculations. Figure 6 shows that strip theory overestimated experiment by about 30 percent. The modified lifting-line theory gave very good agreement with experiment.

CONCLUDING REMARKS

The results of a free-flight investigation of the rolling effectiveness of all-movable horizontal tail fins at a constant differential angle of incidence of 7° per fin indicate that the rolling effectiveness of the all-movable tail was of about the same magnitude at subsonic and supersonic

speeds. The rolling effectiveness of a flexible-wing (fiber-glass—plastic laminate) model was about 1.6 times that of a stiff-wing (solid aluminum alloy) model except in the transonic region.

Langley Aeronautical Laboratory,
        National Advisory Committee for Aeronautics,
                Langley Field, Va., November 12, 1954.

REFERENCES

1. Koenig, David G.: Tests in the Ames 40- by 80-Foot Wind Tunnel of an Airplane Configuration With an Aspect Ratio 3 Triangular Wing and an All-Movable Horizontal Tail — Longitudinal and Lateral Characteristics. NACA RM A52L15, 1953.

2. Sandahl, Carl A., and Marino, Alfred A.: Free-Flight Investigation of Control Effectiveness of Full-Span 0.2-Chord Plain Ailerons at High Subsonic, Transonic, and Supersonic Speeds To Determine Some Effects of Section Thickness and Wing Sweepback. NACA RM L7D02, 1947.

3. Strass, H. Kurt, and Marley, Edward T.: Rolling Effectiveness of All-Movable Wings at Small Angles of Incidence at Mach Numbers From 0.6 to 1.6. NACA RM L51H03, 1951.

4. Diederich, Franklin W., and Zlotnick, Martin: Theoretical Spanwise Lift Distributions of Low-Aspect-Ratio Wings at Speeds Below and Above the Speed of Sound. NACA TN 1973, 1949.
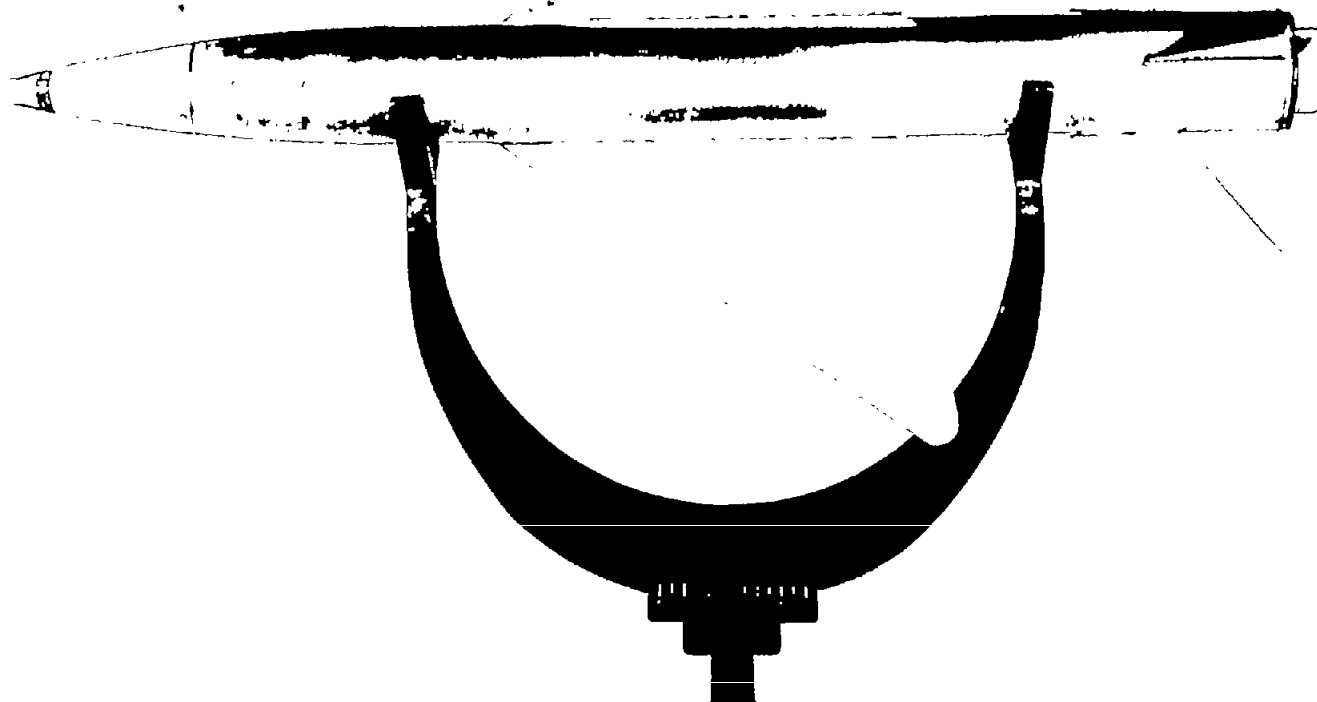
L-83535

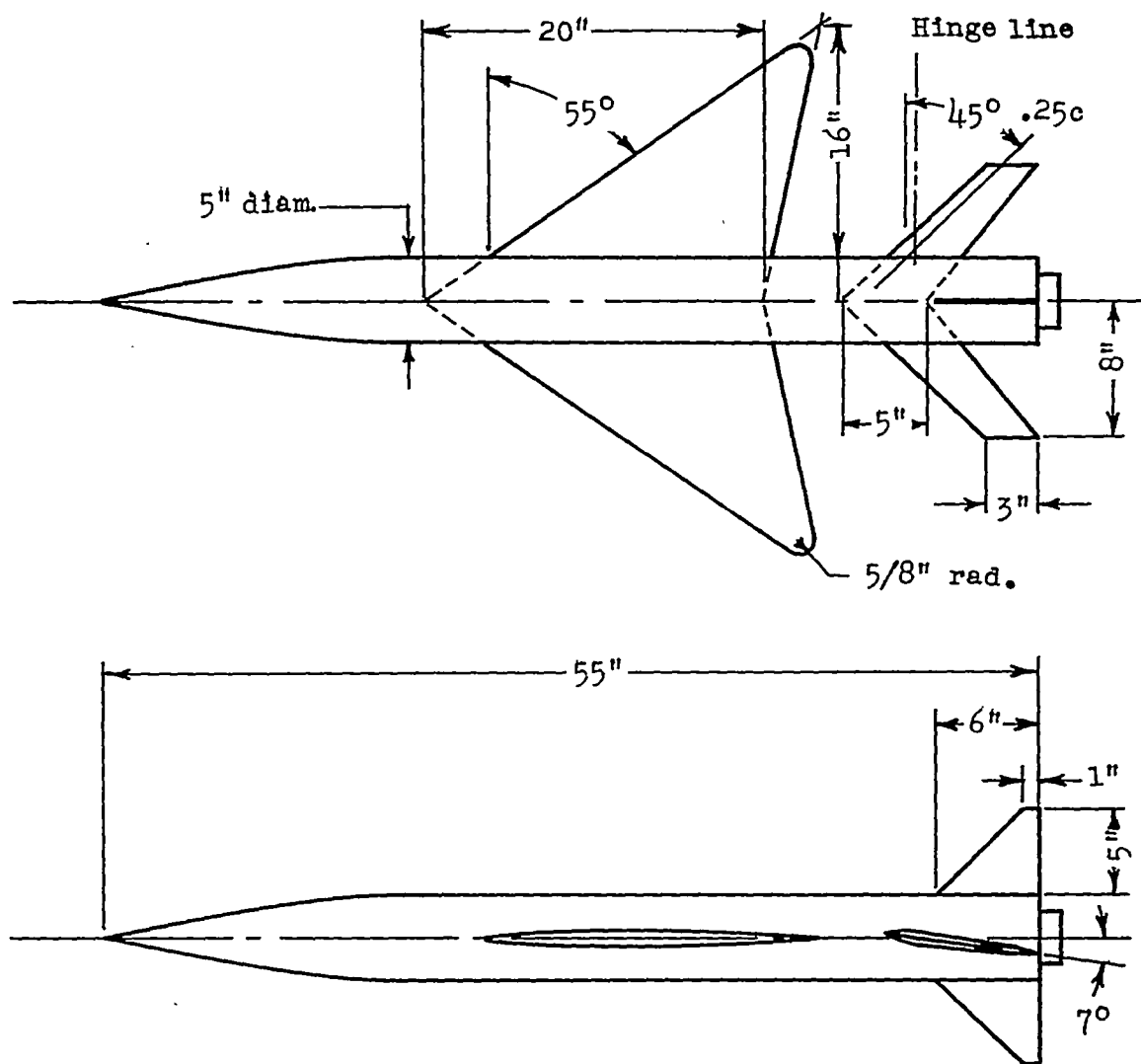Figure 1.- Photograph of test model.
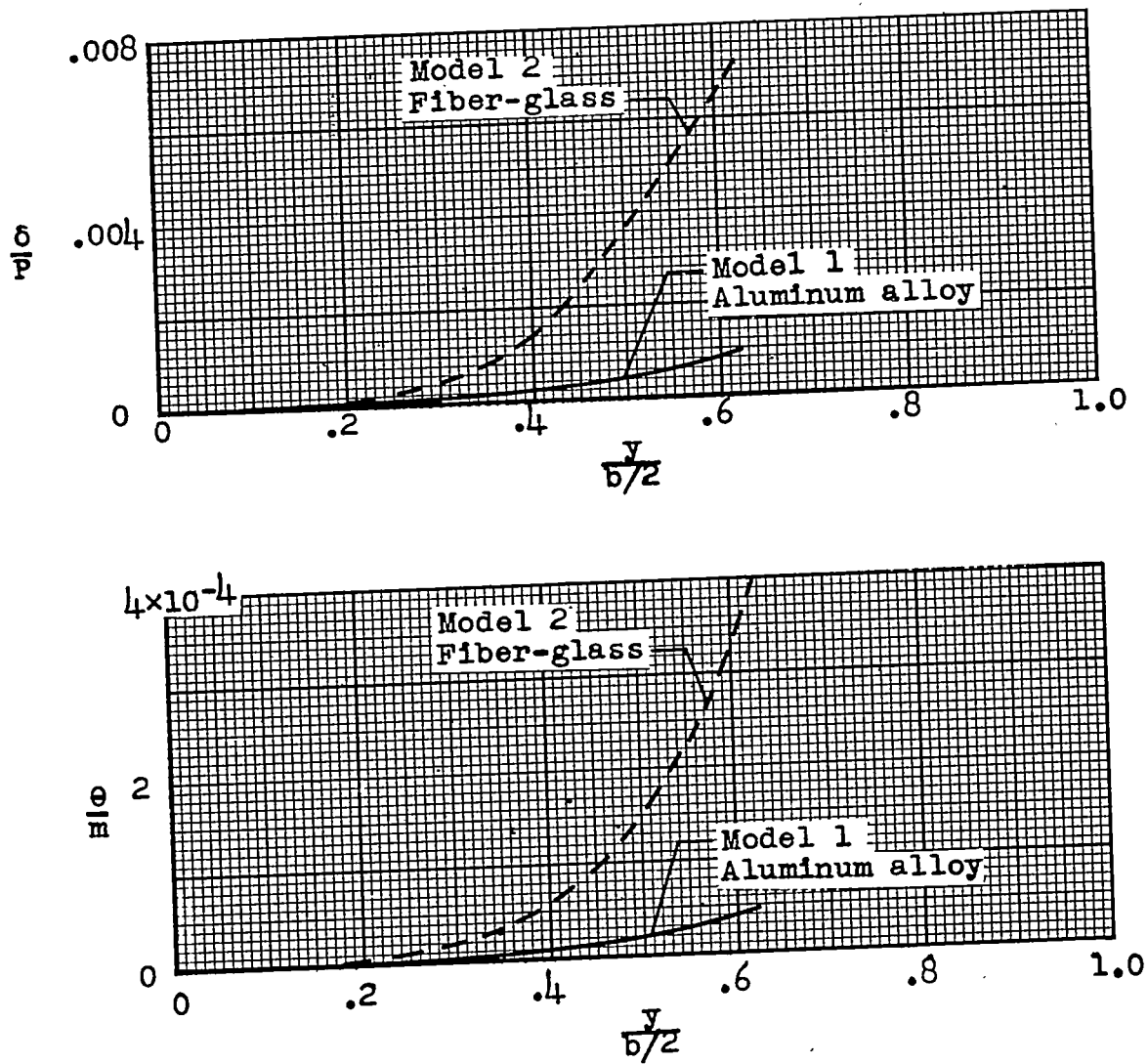
Figure 2.- Sketch of test model.

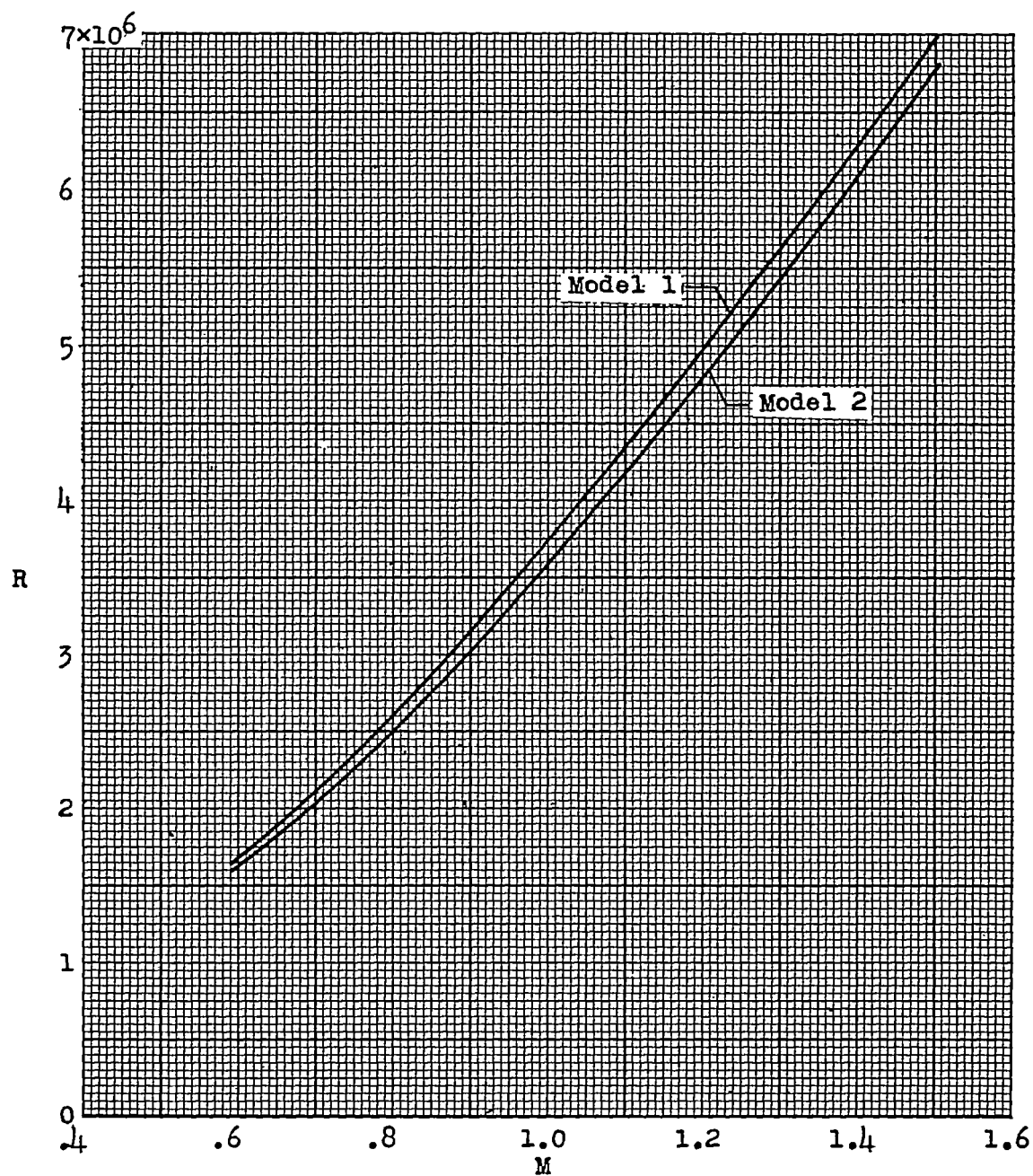Figure 3.- Structural-stiffness characteristics of test wings.

Figure 4.- Variation of Reynolds number with Mach number. Reynolds number based on mean exposed wing chord of 0.703.
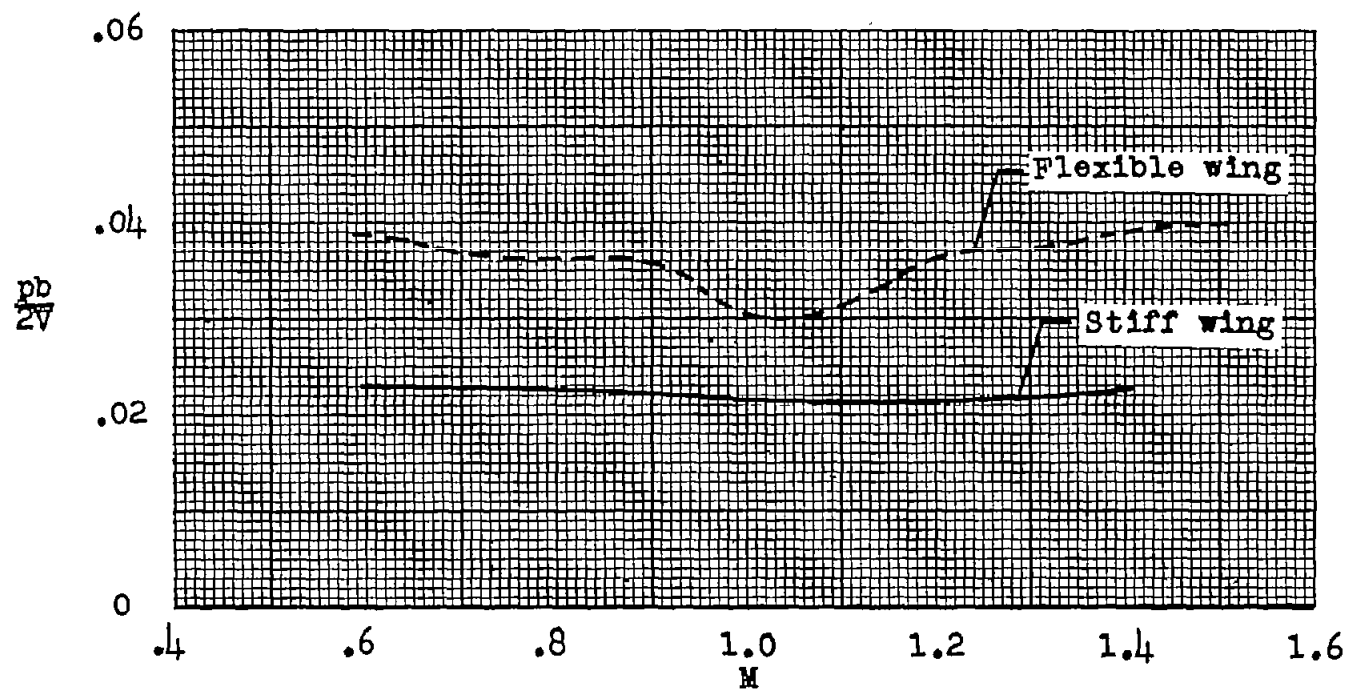
Figure 5.- Variation of the rolling effectiveness parameter pb/2V with
Mach number. i_t = 7°; α = 0°; β = 0°.

$$\frac{pb}{2V}$$

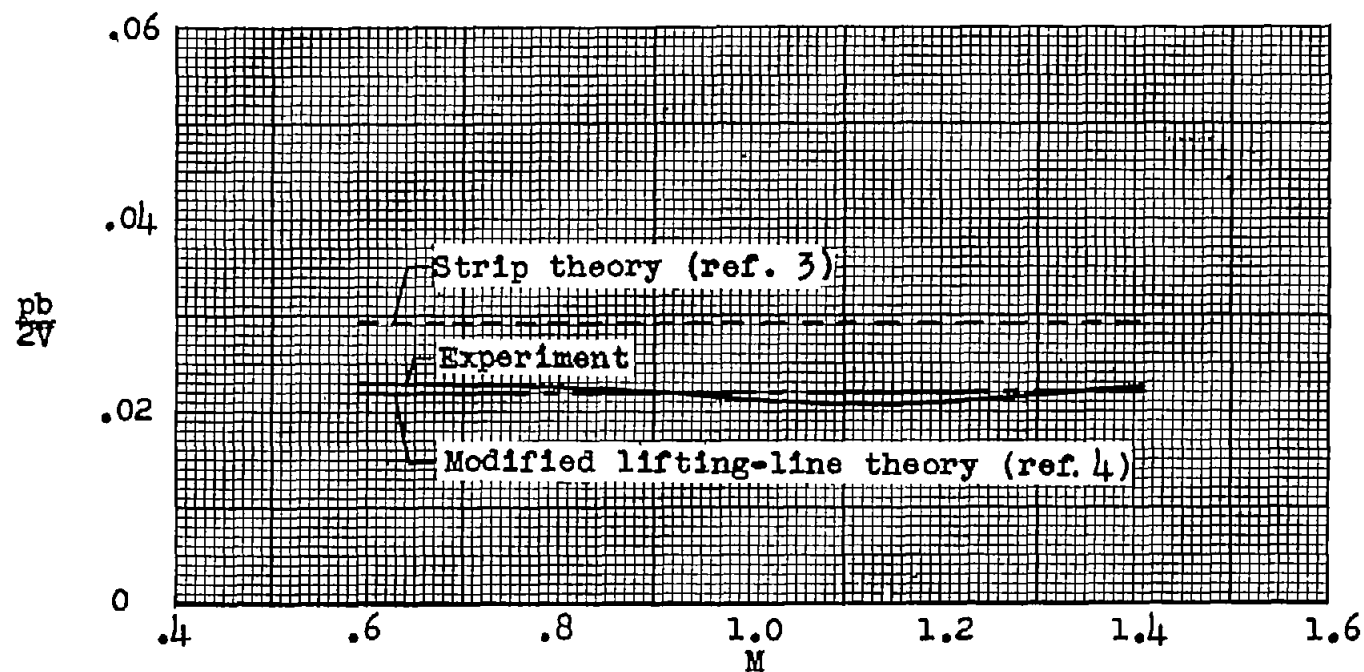Strip theory (ref. 3)

Experiment

Modified lifting-line theory (ref. 4)

Figure 6.- Comparison of experimental and theoretical rolling effective-
ness for the stiff wing. $i_t = 7°$; $\alpha = 0°$; $\beta = 0°$.